



**Faculty of Mechanical Engineering**

**THE ANALYSIS ON FUNCTIONALITY OF COMPOSITE  
SOLDER/OXIDIZE COPPER LEAD FRAME INTERCONNECT IN  
MICROELECTRONIC PACKAGING**

اونيورسيتي تيكنيكل مليسيا ملاك  
UNIVERSITI TEKNIKAL MALAYSIA MELAKA

**Intan Fatimah binti Ahmad**

**Doctor of Philosophy**

**2022**

**THE ANALYSIS ON FUNCTIONALITY OF COMPOSITE SOLDER/OXIDIZE  
COPPER LEAD FRAME INTERCONNECT IN MICROELECTRONIC  
PACKAGING**

**INTAN FATIHAH BINTI AHMAD**

**A thesis submitted  
in fulfillment of requirements for the degree of Doctor of Philosophy**



**Faculty of Mechanical Engineering**

**UNIVERSITI TEKNIKAL MALAYSIA MELAKA**

**2022**

## DECLARATION

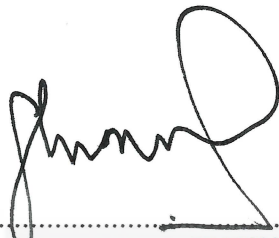
I declare that this thesis entitled “The Analysis on Functionality of Composite Solder/Oxidize Copper Lead Frame Interconnects in Microelectronic Engineering ” is the result of my own research except as cited in the references. The thesis has not been accepted for any degree and is not concurrently submitted in candidature of any other degree.

Signature :   
Name : INTAN FATIMAH BINI AHMAD  
Date : 15/6/2022

اونيورسيتي تيكنيكل مليسيا ملاك  
UNIVERSITI TEKNIKAL MALAYSIA MELAKA

## APPROVAL

I hereby declare that I have read this thesis and in my opinion this thesis is sufficient in terms of scope and quality for the award of Doctor of Philosophy.

Signature : 

Supervisor Name : **PROFESOR IR. TS. DR. GHAZALI BIN OMAR**  
Timbalan Naib Canselor (Penyelidikan & Inovasi)  
Universiti Teknikal Malaysia Melaka

Date : 15/6/2022



اونيورسيتي تيكنيكل مليسيا ملاك  
UNIVERSITI TEKNIKAL MALAYSIA MELAKA

## DEDICATION

*To my husband,*

*Mohd Zulhilmi bin Ismail*

*Who makes me believe everything is possible*

*To my parent,*

*Haji Ahmad bin Abd Razak*

*Hajah Roslizan binti Sulaiman*

*For show me this path and support me every step of the way*

*To my little minions*

*Muhammad Yusuf bin Mohd Zulhilmi*

*Indah Zulaikha binti Mohd Zulhilmi*

*For driving me to never give up*

## ABSTRACT

Recently, the attention toward CNT-composite solder (CCS) has increased remarkably due to numerous advantages. However, the electronic devices' failure is still growing and has become an integral part of the countless product in the industrial market. These failures are mainly related to the reliability of electronic packaging. The significant reliability degradation because the solder has lifted due to the occurrence of the oxide layer on the copper lead frame's surface. Hence, the primary purpose of this study is to analyse the performance of the CCS on the copper lead frame, especially on the oxidise copper lead frame. Nonetheless, the reflow temperature for CCS was first acquired to ensure the uncertainty on data validity could be eliminated. In this study, the commercial solder SAC 305, subjected to different weight percentages (Wt.%), was reflowed on the oxidise copper substrate to analyse the performance of CCS when encountering the oxidise copper lead frame. The CCS subjected to the different weight percentages of carbon nanotube was first characterised to investigate the effect of carbon nanotube on the CCS's properties. Then, the copper lead frame, which undergoes a heat treatment process subjected to four different temperatures (60 °C, 120 °C, 180 °C, and 240 °C), was analysed to ensure the existence of an oxide layer on the copper lead frame's surface. Apart from that, scrutinise the effect of the oxide layer on the copper lead frame's properties. Afterwards, the CCS was reflowed on the oxidise copper lead frame, and the IMC's microstructure of the CCS will be observed through TEM. The CCS is stiffened as the amount of the CNT incorporated into the commercial solder increases. The hardness of the CCS was increased from 15.75 Hv to 17.20 Hv, 17.33 Hv and 18.5 Hv as the wt. % of the CNT increased from 0.01 to 0.02, 0.03 and 0.04. However, the Young modulus for CCS with 0.01 CNT, which is  $3.41 \times 10^{-4}$  N/mm decreased to  $1.5 \times 10^{-4}$  N/mm as the 0.02 wt.% of CNT was added into the solder and increased to  $2.37 \times 10^{-4}$  N/mm and  $4.06 \times 10^{-4}$  N/mm as the 0.03, and 0.04 wt.% was added into the solder. For the oxidising copper lead frame, the native oxide layer already existed on the copper lead frame's surface, and the thickness was 6 nm. The thickness of the oxide layer increased to 10 nm, 19 nm, 110 nm and 350 nm after the copper lead frame was exposed to the temperatures of 60 °C, 120 °C, 180 °C and 240 °C. In addition, the conductivity of the copper lead frame decreased from 58.71 %IACS to 47.2 %IACS and 44.57 %IACS when the copper lead frame was exposed to 60 °C and 120 °C. The conductivity value of the copper lead frame started to increase to 45.41 %IACS and 52.33 %IACS when the copper lead frame was exposed to 180 °C and 240 °C. The presence of the intermetallic compound (IMC) after the CCS reflowed on the oxidise copper lead frame proves that the CCS was successfully joining with the copper lead frame. The void has spotted lies at the surface of the oxidise copper lead frame and along with the IMC layer. The occupancy of voids along the IMC layer will degrade the reliability of the CCS solder. In conclusion, the commercial solder's properties were improved when added with CNT, but the void may develop within the IMC layer when encountered with the oxidise copper lead frame. The void will reduce the life span of the joint. This study's finding profoundly emphasises the knowledge of the CNT-composite solder and when reflowed on the oxidise substrate.

# **ANALISIS FUNGSI KOMPOSIT PATRI/PLUMBUM KUPRUM TEROKSIDA ANTARHUBUNG DALAM PEMBUNGKUSAN MIKROELEKTRONIK**

## **ABSTRAK**

Sejak akhir ini, perhatian terhadap pateri komposit CNT (CCS) telah meningkat dengan ketara. Walau bagaimanapun, kegagalan peranti elektronik masih berkembang dan telah menjadi sebahagian daripada produk yang tidak terkira banyaknya dalam pasaran perindustrian. Kegagalan ini terutamanya berkaitan dengan kebolehpercayaan pembungkusan elektronik. Kemerosotan kebolehpercayaan yang ketara kerana pateri telah terangkat akibat adanya lapisan oksida pada permukaan rangka plumbum kuprum. Oleh itu, tujuan utama kajian ini adalah untuk menganalisis prestasi CCS pada rangka plumbum kuprum, terutamanya pada rangka plumbum kuprum teroksida. Namun begitu, 'reflow temperature' untuk CCS perlu diperoleh dahulu untuk memastikan keraguan terhadap kesahihan data dapat dihapuskan. Dalam kajian ini, pateri komersil SAC 305, dengan peratusan berat yang berbeza (Wt.%), dipateri pada substrat kuprum teroksida untuk menganalisis prestasi CCS apabila dipateri pada bingkai plumbum kuprum teroksida. CCS dengan peratusan berat berbeza CNT akan dianalisis terlebih dahulu untuk menyiasat kesan CNT pada sifat CCS. Kemudian, kerangka plumbum kuprum, yang menjalani proses rawatan haba tertakluk kepada empat suhu berbeza (60 °C, 120 °C, 180 °C dan 240 °C), dianalisis untuk memastikan kewujudan lapisan oksida pada permukaan rangka plumbum kuprum. Selain itu, kesan lapisan oksida terhadap sifat rangka plumbum kuprum juga akan dikaji. Selepas itu, CCS akan dipateri pada bingkai plumbum kuprum teroksida, dan struktur IMC bagi CCS akan diperhatikan melalui TEM. CCS menjadi semakin kuat apabila jumlah CNT yang digabungkan ke dalam pateri komersial meningkat. Kekerasan CCS meningkat daripada 15.75 Hv kepada 17.20 Hv, 17.33 Hv dan 18.5 Hv apabila wt.% daripada CNT meningkat daripada 0.01 kepada 0.02, 0.03 dan 0.04. Walau bagaimanapun, 'Young Modulus' untuk CCS dengan campuran 0.01 CNT, iaitu  $3.41 \times 10^{-4}$  N/mm menurun kepada  $1.5 \times 10^{-4}$  N/mm apabila 0.02 wt.% CNT telah ditambah ke dalam pateri dan meningkat kepada  $2.37 \times 10^{-4}$  N/mm dan  $4.06 \times 10^{-4}$  N/mm sebagai 0.03, dan 0.04 wt.% telah ditambah ke dalam pateri. Untuk bingkai plumbum kuprum pengoksidaan, lapisan oksida tersedia ada pada permukaan bingkai plumbum kuprum, dengan ketebalannya ialah 6 nm. Ketebalan lapisan oksida meningkat kepada 10 nm, 19 nm, 110 nm dan 350 nm selepas rangka plumbum kuprum didedahkan kepada suhu 60 °C, 120 °C, 180 °C dan 240 °C. Selain itu, kekonduksian rangka plumbum kuprum menurun daripada 58.71 %IACS kepada 47.2 %IACS dan 44.57 %IACS apabila rangka plumbum kuprum didedahkan kepada 60 °C dan 120 °C. Nilai kekonduksian rangka plumbum kuprum mula meningkat kepada 45.41 %IACS dan 52.33 %IACS apabila bingkai plumbum kuprum didedahkan kepada 180 °C dan 240 °C. Kehadiran sebatian antara logam (IMC) selepas CCS dipateri pada rangka plumbum kuprum teroksida membuktikan bahawa CCS berjaya bercantum dengan bingkai plumbum kuprum. 'Void' telah kelihatan wujud pada permukaan bingkai plumbum kuprum teroksida dan juga sepanjang lapisan IMC. 'Void' yang ada di sepanjang lapisan IMC akan merendahkan kebolehpercayaan pateri CCS. Kesimpulannya, sifat pateri komersial telah dipertingkatkan apabila ditambah dengan CNT, tetapi 'void' boleh wujud dalam lapisan IMC 'Void' ini akan mengurangkan jangka hayat pateri. Penemuan kajian ini menambahkan lagi pengetahuan berkenaan tentang pateri komposit CNT dan sifat CCS apabila dipateri pada substrat pengoksidaan.

## ACKNOWLEDGEMENT

All praise to Allah S.W.T. The Almighty God for the strength and mercy upon me in completing this research degree.

This thesis also becomes a reality with many individuals' kind support and help. I want to extend my sincere thanks to all of them.

First and foremost, I would like to express my sincere gratitude to my primary supervisor Profesor Ir. Dr. Ghazali bin Omar for his guidance, patience, support and knowledge that enabled me to complete this research degree successfully. I would also like to convey my appreciation to Ir. Ts. Dr. Mohd Azli bin Salim as my second supervisor.

Special thanks to all staff and colleagues from Advanced Material Characterization Lab (AMCHAL) for all technical support and assistance throughout my studies.

Last but not least, I would like to send my love and appreciation to my family, especially my husband, Mohd Zulhilmi bin Ismail for his love, moral and financial support, and encouragement throughout this research degree.



## TABLE OF CONTENT

	PAGE
<b>DECLARATION</b>	
<b>APPROVAL</b>	
<b>DEDICATION</b>	
<b>ABSTRACT</b>	<b>i</b>
<b>ABSTRAK</b>	<b>ii</b>
<b>ACKNOWLEDGEMENT</b>	<b>iii</b>
<b>TABLE OF CONTENT</b>	<b>iv</b>
<b>LIST OF TABLES</b>	<b>vii</b>
<b>LIST OF FIGURES</b>	<b>ix</b>
<b>LIST OF ABBREVIATIONS</b>	<b>xvi</b>
<b>LIST OF PUBLICATIONS</b>	<b>xviii</b>
<b>CHAPTER</b>	
<b>1. INTRODUCTION</b>	<b>1</b>
1.1 Overview	1
1.2 Problem statement	4
1.3 The objective of the research	6
1.4 Scope and limitations	6
1.5 Outlines of the research	7
<b>2. LITERATURE REVIEW</b>	<b>9</b>
2.1 Introduction to soldering technology	9
2.1.1 Microstructure and intermetallic layer formation of SAC305/Cu substrate	17
2.1.2 Mechanical properties of lead-free solder	23
2.2 Composite Solder	38
2.2.1 Fabrication of the composite solder	40
2.2.1.1 Mechanical mixing method	40
2.2.1.2 The <i>in-situ</i> method	41
2.3 Copper lead frame in semiconductor packaging	43
2.2.1 Oxidation of copper lead-frame	46
2.4 Summary and Research Gap	51
<b>3. METHODOLOGY</b>	<b>54</b>
3.1 Raw materials	57
3.1.1 Solder alloy SAC305 material	57
3.1.2 Carbon nanotube (CNT) material	59
3.1.3 Printed Circuit Board (PCB)	60
3.1.4 Copper Lead Frame	61
3.2 Sample preparation	62
3.2.1 Preparation of CCS with different wt.% of CNT	63
3.2.2 Design and fabrication of PCB	66
3.2.2.1 UV curing process	67
3.2.2.2 Developing process	69
3.2.2.3 Etching process	71
3.2.2.4 Photoresist stripper process	72
3.2.3 The process of promoting oxide layer on Copper Lead-Frame	74

3.2.4	The process to deposit CCS on PCB and C194	76
3.3	Sample characterization	78
3.3.1	Cross-section method	78
3.3.1.1	Mechanical cross-section	79
3.3.1.2	Cross-section through cross-section polisher (CP)	81
3.3.2	Thermal characterization by using Differential Scanning Calorimetry (DSC)	83
3.3.3	Surface roughness characterization by Atomic Force Microscopy (AFM)	84
3.3.4	Mechanical characterization by using Dynamic Ultra Micro Hardness Tester	85
3.3.5	Morphological characterization	87
3.3.5.1	Morphological observation by using Upright Microscope	87
3.3.5.2	Morphological observation by Scanning Electron Microscopy (SEM)	88
3.3.5.3	Morphological observation by Transmission Electron Microscopy (TEM)	89
3.3.6	Depth profiling analysis by Auger Electron Spectroscopy (AES)	90
3.3.7	Resistivity measurement by using a four-point probe	91
3.3.7.1	The resistivity of solder alloy and composite Solder	91
3.3.6.1	The resistivity of the copper lead-frame	92
<b>4.</b>	<b>RESULT AND DISCUSSIONS</b>	<b>95</b>
4.1	Reflow profile of CNT-composite solder (CCS)	96
4.1.1	DSC measurements on SAC305 and CCS solder	96
4.1.2	Ideal duration of exposure reflow temperature for CCS reflow profile	101
4.1.3	Summary of CCS reflow profile	110
4.2	Effects of reinforcing the CNT on intermetallic growth and hardness of SAC305 solder alloy	110
4.2.1	The microstructure and intermetallic compound's growth of the SAC305 solder alloy and the CCS solder	111
4.2.2	Mechanical properties of solder SAC305 with different percentages of CNT	115
4.2.2.1	The hardness and Young modulus of the SAC305 and all CCS solder	116
4.2.2.2	The grain size of the SAC305 and all CCS Solder	118
4.2.3	Summary on the effect of wt.% CNT toward composite Solder	124
4.3	Effect of oxidation on the copper lead frame's properties	125
4.3.1	Effectiveness of the heat-treatment process to promote oxidation on the copper lead frame's surface	126
4.3.2	Effect of oxidation on properties of the copper lead frame	137
4.3.2.1	Electrical properties of oxidizing copper lead-frame	137

4.3.2.2	Mechanical properties of oxidizing copper lead-frame	141
4.3.3	Summary of oxidation effect on copper lead frame's properties	146
4.4	Performance of composite solder on oxidation copper lead-frame	147
4.4.1	Interfacial reactions between composite solder and oxidation cu lead-frame	148
4.4.2	The evolution of the IMC's roughness	155
4.4.3	The relation between the void's formation and the IMC layer	159
4.4.4	Summary of the effect of the oxidized copper lead frame On composite solder's performance	165
<b>5.</b>	<b>CONCLUSION AND RECOMMENDATIONS</b>	<b>166</b>
5.1	Conclusion of the research	166
5.2	Contribution to Knowledge and Science	168
5.3	Recommendation for future study	168
	<b>REFERENCES</b>	<b>170</b>



## LIST OF TABLES

TABLE	TITLE	PAGE
2.1	List of etching solution for a different type of solder	23
2.2	Summary of mechanical testing on Pb-free solder from previous researchers	31
2.3	Typical reinforcement type in composite solder research	39
3.1	Recommendation value at each profile phase	59
3.2	Detail information on wt.% of CNT and SAC305	64
3.3	The detail on exposure temperature and duration of the treatment	75
3.4	The correction factor (G) table	94
4.1	Solidus, liquidus, and melting range of the SAC305 solder alloy and CCS	98
4.2	Thermal properties of SAC305 solder alloy and CCS	100
4.3	Summary findings of experiment on different times of reflow temperature	109
4.4	Details information on reflow profile used on CCS solder	110
4.5	Diffusion coefficient (D) of SAC305 and CCS solder	114
4.6	Hardness and Young modulus of the SAC305 solder and all CCS solder	117
4.7	The grain size value for SAC305 and all CCS solder	119
4.8	The EDX spectrum results for SAC305 and all CCS solder	124

4.9	Table summary of the CNT-composite solder properties	125
4.10	Details of weight % and atomic % for Sample A, Sample B, Sample C, Sample D, and Sample E	130
4.11	The sheet resistivity, volume resistivity, and conductivity of all samples	137
4.12	Summary properties of oxide copper lead-frame	147



## LIST OF FIGURES

FIGURE	TITLE	PAGE
2.1	Hierarchy level of interconnection in semiconductor packaging	10
2.2	Wire bonding interconnect in quadruplet flat package (QFP)	11
2.3	Image of bottom BGA and cross-section of BGA	12
2.4	The cross-section of the flip-chip ball grid array (FCBGA)	12
2.5	Hand soldering for through-hole technology	13
2.6	Example of wave soldering during through-hole technology	14
2.7	Classification of reflow profile with (a) Details profile feature for SnPb solder and Lead-free solder (b) standard reflow profile graph	16
2.8	Phase diagram of SnPb solder	18
2.9	The lamellar structure for SnPb solder	18
2.10	Illustration of the interfacial reaction of SAC305 with Cu substrate during the reflow process	20
2.11	The formation of IMC during the reflow process	20
2.12	Phase diagram of the binary system (a) Sn-Ag (b) Sn-Cu	21
2.13	Example microstructure of SAC305	22
2.14	Schematic indentation of Vickers tip (four-sided pyramid), Brinell tip (spherical tip), and Berkovich tip (three-sided pyramid)	24
2.15	Load-displacement curve based on the Oliver and Pharr method	30
2.16	Example of a copper lead frame with different geometry	45

2.17	Example delamination of IC package	46
2.18	Illustration of die-attach using conductive adhesive or silver glass material	47
2.19	Illustration of the die-attach process using eutectic solder	48
2.20	Example of die-attach materials with operation ranges, temperature ranges, and possibilities category	49
2.21	Research gap of this study (different wt.% of CNT)	52
2.22	Research gap of this study (different exposure temperature to promote oxidation process)	53
3.1	Flow chart of research methodology	54
3.2	Process flow of phase one	55
3.3	Process flow of phase two	56
3.4	Process flow of phase three	57
3.5	The image of solder type SAC305	58
3.6	The SEM image of solder powder	58
3.7	Recommendation reflow profile graph	59
3.8	SEM image of multiwalled carbon nanotube (MWCNT)	60
3.9	The image of the printed circuit board (PCB) (a) with the surface covered by the green sticker (b) bare positive board	61
3.10	The image of the as-received C194	61
3.11	Sample preparation's process by using PCB as the substrate	63
3.12	Sample preparation's process by using copper lead-frame as the substrate	63
3.13	Image of Thinky mixer machine (ARE-310)	65
3.14	Process flow of CCS preparation	65

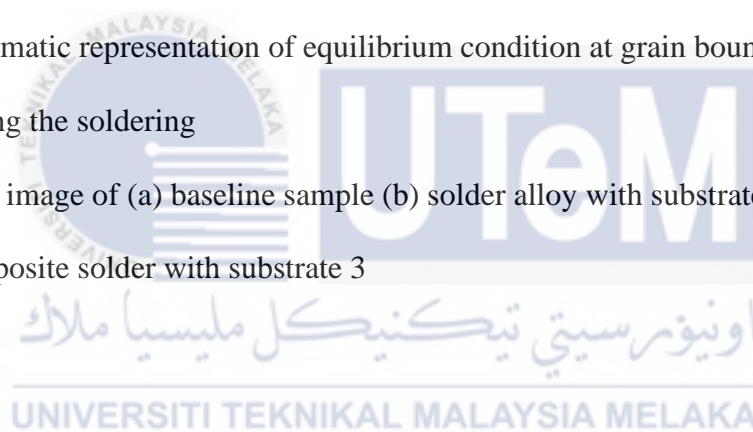
3.15	CCS with (a) 0.01 wt.% of CNT (b) 0.02 wt.% of CNT (c) 0.03 wt.% of CNT (d) 0.04 wt.% of CNT	66
3.16	Flow of PCB fabrication process	67
3.17	The accublack paper with dot pattern	67
3.18	UV curing machine	68
3.19	Illustration of the UV curing process	69
3.20	PCB developer machine with (a) Front view of PCB developer machine (b) PCB soaked into the water tank	70
3.21	Illustration of softening positive photoresist had been washed away by a developer solution	70
3.22	Etching machine	71
3.23	Illustration of copper was etched during the etching process	72
3.24	PCB image (a) before etching process (b) after etching process	72
3.25	Photoresist stripper (a) machine (b) the PCB soaked into the photoresist solution	73
3.26	Illustration of the positive layer removal during the photoresist stripper process	74
3.27	Image of PCB with Copper dot	74
3.28	Image of laboratory oven used to heat the copper	75
3.29	Syringe dispensing of soldering (a) during dispensing soldering (b) Cu substrate of PCB filled with solder	76
3.30	Reflow process (a) Reflow oven machine (b) position of PCB before inserting into Reflow oven	77
3.31	Reflow profile for CNT-composite solder	77
3.32	The image of the final sample	78

3.33	Image of the (a) Epoxy resin and (b) Hardener	79
3.34	The condition of the solder sample in the mounting cup (a) the sample in the mounting cup (b) Final product of cold mount sample	80
3.35	Mechanical cross-section process (a) Image of grinder and polisher machine (b) close up image of grinder base during cross-section process	81
3.36	Ion Polisher machine	82
3.37	Illustration of ion beam irradiated the sample	82
3.38	Sample placement (a) on IP sample mounting (b) Side view of the sample	83
3.39	Image of Atomic Force Microscopy equipment	85
3.40	Image of (a) Dynamic Ultra Micro Hardness equipment (b) Enlargement of the sample placement area	86
3.41	Upright microscope equipment	88
3.42	Image of (a) SEM machine (b) Sputter coater machine	89
3.43	Image of TEM machine	90
3.44	Four-point probe equipment	92
3.45	Illustration of the four-point probe principle	92
3.46	Illustration of the copper lead-frame	93
4.1	The DSC profile of solder SAC305	97
4.2	Endothermic graph of SAC305 and CCS solder	98
4.3	Illustration of (a) intermolecular force within a solder alloy system and (b) intermolecular force within composite solder system	100
4.4	Three profile with difference duration of reflow time (a) 60s (b) 105s (c) 150s	103

4.5	Top view of 0.04-CCS after using (a) profile 1 (b) profile 2 (c) profile 3	104
4.6	Illustration of the tiny ball appeared after the reflow process	105
4.7	Contact angle measurement for 0.04-CCS reflow under (a) profile 1 (b) profile 2 (c) profile 3	107
4.8	Backscatter image of 0.04-CCS with (a) sample 1 (b) sample 2 (c) sample 3	108
4.9	SEM images (back-scattered electron microscopy) of IMC for (a) SAC305 (b) 0.01-CCS (c) 0.02-CCS (d) 0.03-CCS (e) 0.04-CCS	112
4.10	Thickness of IMC versus percentage of CNT	114
4.11	Illustration of interaction between Sn atoms and Cu atoms	115
4.12	Force-displacement graph (P-h) of SAC305 and all CCS solder	117
4.13	The polished surface of (a) SAC305 (b) 0.01-CCS (c) 0.02-CCS (d) 0.03-CCS (e) 0.04-CCS with different grain size	120
4.14	Illustration of CNT entrapped within the solder matrix	122
4.15	The SEM image of (a) SAC305 (b) 0.01-CCS (c) 0.02-CCS (d) 0.03- CCS and (e) 0.04-CCS showing black particles along the grain boundary	123
4.16	SEM image of the solder 0.04-CCS (a) with 50x magnification (b) with 1000x magnification	124
4.17	The optical image of lead frame (a) sample A (b) sample B (c) sample C	127
4.18	Surface roughness of sample A, sample B, sample C, sample D, and sample E	128
4.19	Micrograph of AFM for copper lead-frame (a) Sample A, (b) Sample	130

	B, (c) Sample C, (d) Sample D, and (e) Sample E	
4.20	EDX results on (a) sample A (b) sample B (c) sample C (d) sample D and (e) sample E	131
4.21	Atomic percentage of oxygen variable versus temperature of heat treatment	132
4.22	The Auger depth profiling graph and the TEM image of the copper lead frame after undergoes temperature at (a,b) sample A (c,d) sample B (e,f) sample C (g,h) sample D and (i,j) sample E	136
4.23	Conductivity and Sheet resistance of sample A, sample B, sample C, sample D, and sample E	138
4.24	The graph of conductivity of all sample versus thickness of the copper oxide	139
4.25	Graph of copper lead frame's hardness versus heat treatment's temperature	142
4.26	Force-displacement graph for a copper lead frame before and after heat treatment	143
4.27	The relationship graph between the type of sample with hardness, young modulus, and thickness of copper oxide	144
4.28	Surface microstructure of copper lead frame at (a) sample A (b) sample B (c) sample C (d) sample D and (e) sample E	146
4.29	SEM image of IMC for SAC305 solder alloy reflowed on (a) substrate 1 (c) substrate 2 (e) substrate 3 and SEM image of IMC for CCS reflowed on (b) substrate 1, (d) substrate 2 and (f) substrate 3	149
4.30	The graph of type of substrate against SAC305 and CCS IMC thickness	150

4.31	The graph of Diffusion coefficient for both SAC305 and CCS on three different substrates	153
4.32	Illustration of the copper atom breaking the oxide layer to interact with the Sn atom	153
4.33	Illustration of interaction between the CNT and CuO has open the path of the copper and Sn	155
4.34	The graph of surface roughness (Ra) of SAC305 solder alloy and CCS's IMC layer	156
4.35	Schematic diagram of Ra and Mean Surface level (MSL) at the solder/Cu <sub>6</sub> Sn <sub>5</sub> interface	157
4.36	Schematic representation of equilibrium condition at grain boundaries during the soldering	158
4.37	IMC image of (a) baseline sample (b) solder alloy with substrate 3 (c) composite solder with substrate 3	161



## LIST OF ABBREVIATIONS

AFM	-	Atomic Force Microscopy
BGA	-	Ball Grid Array
CNT	-	Carbon nanotube
CP	-	Cross-section Polisher
DIP	-	Dual in-line Package
DSC	-	Differential Scanning Calorimetry
FCBGA	-	Flip Chip Ball Grid Array
I/O	-	Input Output
IDEALS	-	Improve Design life and Environmentally aware manufacturing of Electronic assemblies by Lead-free soldering
IMC	-	Intermetallic Compound
iNEMI	-	International Electronics Manufacturing Initiative
JEITA	-	Japan Electronics and Information Technology Industries Association
LFSP	-	Lead Free Solder Project
MSDS	-	Material Safety Data Sheet
MWCNT	-	Multiwalled Carbon Nanotube
NCMS	-	National Centre for Manufacturing Sciences
PCB	-	Printed Circuit Board
PGA	-	Pin Grid Array
ROHS	-	Restriction of Hazardous Substances
QFD	-	Quadruplet flat package
SAC	-	Sn Ag Cu
SEM	-	Scanning Electron Microscopy

- SMT - Surface Mount Technology  
TAL - Temperature Above Liquidus  
THT - Through Hole Technology  
UV - Ultra-Violet



## LIST OF PUBLICATIONS

### Paper 1

Ahmad, I.F., Omar, G. and Salim, M.A., 2018. Extrinsic Activation Energy for Enhanced Solid-State Metallic Diffusion for Electrical Conductive Ink. *Journal of Advanced Research in Fluid Mechanics and Thermal Sciences*, 50(1), pp.32-39.

### Paper 2

Ahmad, I. F., Omar, G., Hamid, H. A. and Salim, M. A., 2021. Effect of Carbon Nanotube on Microstructure and Hardness of Sn96.5Ag3.0Cu0.5 Solder for Microelectronic Packaging. *Journal of International Review of Mechanical Engineering*, 15(7).



# CHAPTER 1

## INTRODUCTION

This chapter provides information regarding the study's background, problem statements, objectives, research questions, scope and limitations, and the potential benefits. This chapter also presents an outline of how the investigation has been carried out.

### 1.1 Overview

Semiconductor devices such as integrated circuits (ICs) are ubiquitous in electronic devices. The device can act as an amplifier, oscillator, microprocessor, or even a timer and can be found in automobiles, computers, aerospace, and trains (Ng et al., 2016; Sangantrakul and Wongsawat, 2018; Shirriff, 2016; Yu et al., 2019). The ICs are fabricated as a single unit, consisting of the silicon die, and placed on the lead frame by the die-attach process. The silicon die consists of multiple individual components such as transistors, diodes, and capacitors connected by the conductive pathway (Chia et al., 2018). The lead frame, typically a copper alloy, is used as the package's skeleton, where different components are laid to form a complete package (Esa et al., 2017). Although ICs are becoming much more prevalent, they are still commonly packaged with lead frame components.

Meanwhile, the die-attach bond is a process of affixing the silicon die to the lead frame by using adhesive, conductive adhesive, or solder. Most ICs are subjected to variations of temperature during operation. Thus it is essential to intensely dissipate the thermal energy (Mohamed et al., 2019). The solder is the most promising material to be used during the die-attach process, especially for power devices or during the rapid mounting of inexpensive